How CSMA/CA With Deferral Affects Performance and Dynamics in Power-Line Communications

Christina Vlachou, Albert Banchs, *Senior Member, IEEE*, Julien Herzen, and Patrick Thiran, *Fellow, IEEE*

***Abstract*— Power-line communications (PLC) are becoming a key component in home networking, because they provide easy and high-throughput connectivity. The dominant MAC protocol for high data-rate PLC, the IEEE 1901, employs a CSMA/CA mechanism similar to the backoff process of 802.11. Existing performance evaluation studies of this protocol assume that the backoff processes of the stations are independent (the so-called decoupling assumption). However, in contrast to 802.11, 1901 stations can change their state after sensing the medium busy, which is regulated by the so-called deferral counter. This mechanism introduces strong coupling between the stations and, as a result, makes existing analyses inaccurate. In this paper, we propose a performance model for 1901, which does not rely on the decoupling assumption. We prove that our model admits a unique solution for a wide range of configurations and confirm the accuracy of the model using simulations. Our results show that we outperform current models based on the decoupling assumption. In addition to evaluating the performance in steady state, we further study the transient dynamics of 1901, which is also affected by the deferral counter.**

***Index Terms*— HomePlug, power-line communications (PLC), deferral counter, CSMA/CA, decoupling assumption.**

I. Introduction

POWER-LINE communications (PLC) are increasingly important in home networking. HomePlug, the most popular specification for PLC, is employed by over 180 million devices worldwide [2], and offers data rates up to 1.5 Gbps. Moreover, PLC plays an important role in hybrid networks comprising wireless, Ethernet, and other technologies [3], as it contributes to increasing the bandwidth of such networks with an independent, widely accessible medium. Yet, despite the wide adoption of HomePlug specifications in home networks, little attention has been paid to providing an accurate analysis and an evaluation of the HomePlug MAC layer.

Manuscript received February 25, 2015; revised October 21, 2015 and April 22, 2016; accepted May 21, 2016; approved by IEEE/ACM TRANSACTIONS ON NETWORKING Editor S. Chong. This work was supported by the Hasler Stiftung, Bern, Switzerland, through the SmartWorld Project. The work of A. Banchs was supported by the Spanish Ministry of Economy and Competitiveness within the THWART Project under Grant TEC2015-70836-ERC. This work was performed while A. Banchs was visiting EPFL. This paper is an extended version of the paper "On the MAC for Power-Line Communications: Modeling Assumptions and Performance Tradeoffs" [1], which was presented at IEEE ICNP 2014 and has earned the Best Paper Runner Up Award.

C. Vlachou and P. Thiran are with the École Polytechnique Fédérale de Lausanne, Lausanne 1015, Switzerland (e-mail: christina.vlachou@epfl.ch; patrick.thiran@epfl.ch).

A. Banchs is with IMDEA Networks Institute and the University Carlos III of Madrid, Leganés 28911, Spain (e-mail: banchs@it.uc3m.es).

J. Herzen is with Swisscom, Bern 3006, Switzerland (e-mail: julien.herzen@swisscom.com).

Color versions of one or more of the figures in this paper are available online at http://ieeexplore.ieee.org.

Digital Object Identifier 10.1109/TNET.2016.2580642

The vast majority of HomePlug devices employ a multiple-access protocol based on CSMA/CA that is specified by the IEEE 1901 standard [4]. This CSMA/CA mechanism resembles the CSMA/CA mechanism employed by IEEE 802.11, but with important differences in terms of complexity, performance and fairness. The main difference stems from the introduction of a so-called *deferral counter* that triggers a redraw of the backoff counter when a station *senses the medium busy*. This additional counter significantly increases the state-space required to describe the backoff procedure. Moreover, as we explain in more details later, the use of the deferral counter introduces some level of coupling between the stations, which penalizes the accuracy of models based on the *decoupling assumption*. This assumption was originally proposed in the 802.11 analysis of [5] and has been used in all works that have analyzed the 1901 CSMA/CA procedure so far (i.e., [6]–[8]). In this paper, we show that this decoupling assumption leads to inaccurate results, and the modeling accuracy can be substantially improved by avoiding it.

The decoupling assumption relies on the approximation that the backoff processes of the stations are independent and that, as a consequence, stations experience the same time-invariant collision probability, independently of their own state and of the state of the other stations [5]. In addition, to analyze 1901, it has been assumed that a station senses the medium busy with the same time-invariant probability (equal to the collision probability) at any time slot [6], [7]. In this paper, we show that the deferral counter introduces some coupling among the stations: After a station gains access to the medium, it can retain it for many consecutive transmissions before any other station can transmit. As a result, the collision and busy probabilities are not time-invariant for 1901 networks, which makes the decoupling assumption questionable.

Figure 1 provides some evidence of the coupling phenomenon described above, for a HomePlug AV testbed with two stations. While Station A transmits during several consecutive slots, Station B is likely to remain in a state where it has a higher probability of colliding or sensing the medium busy. B is then even less likely to attempt a transmission while in this state, and it might have to wait several tens of milliseconds before the situation reverts. Thus, the collision probabilities observed by the stations are clearly time-varying, which invalidates the decoupling assumption.

In this paper, we propose a theoretical framework to model the CSMA/CA process of 1901 without relying on the decoupling assumption. We first introduce a model that considers the coupling between stations and accurately captures 1901 performance. This model is relatively compact: com-

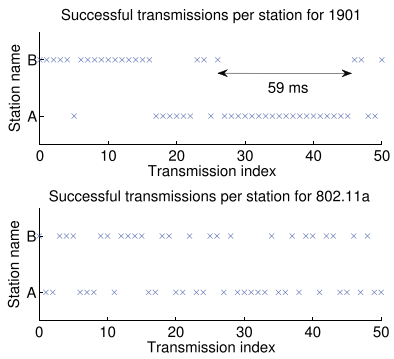

Fig. 1. Testbed trace of 50 successful transmissions by two saturated stations with 1901 and 802.11a. 1901 exhibits short-term unfairness: a station holding the channel is likely to keep holding it for many consecutive transmissions, which causes high dependence between the stations. 802.11 is fairer, which makes the decoupling assumption viable in this case.

puting the throughput of the network only requires to solve a system of m non-linear equations, where m is the number of backoff stages (the default value for 1901 is $m = 4$). We then prove that this system of equations admits a unique solution. We confirm the accuracy of the model by using both simulations and a testbed of 7 HomePlug AV stations. In addition, we investigate the accuracy of our model and that of previous works relying on the decoupling assumption, showing that ours is the first model for 1901 reaching this level of accuracy.

The remainder of the paper is organized as follows. We present the 1901 backoff process in Section II. We then review the related work on MAC layer in Section III. We present our model for 1901 and discuss the system dynamics in Section IV. We evaluate the performance of our model and discuss the decoupling assumption in Section V. Finally, we give concluding remarks in Section VI.

II. The CSMA/CA Protocol of IEEE 1901

We describe the main features of the CSMA/CA protocol used in 1901 [4]. We highlight in particular the mechanism that causes the strong coupling between stations and that is the main difference between 1901 and 802.11.

The 1901 CSMA/CA procedure includes two counters: the backoff counter (BC) and the deferral counter (DC). Upon the arrival of a new packet, a transmitting station enters backoff stage 0. It then draws the backoff counter BC uniformly at random in $\{0, \ldots, CW_0 - 1\}$, where CW_0 denotes the contention window used at backoff stage 0. Similarly to 802.11, BC is decreased by 1 at each time slot if the station senses the medium to be idle (i.e., below the carrier-sensing threshold), and it is frozen when the medium is sensed busy. In the case the medium is sensed busy, BC is also decreased by 1 once the medium is sensed idle again. When BC reaches 0, the station attempts to transmit the packet. Also similarly to 802.11, the station jumps to the next backoff stage if the transmission fails. In this case, the station enters the next backoff stage. The station then draws BC uniformly at random in $\{0, \ldots, CW_i - 1\}$, where CW_i is the contention window used for backoff stage i, and repeats the process. For 802.11, the contention window is doubled between the successive backoff stages, i.e., $CW_i = 2^i CW_0$. For 1901, CW_i depends on the value of the backoff stage i and the priority of the packet: There are four backoff stages, as given in Table I. Also, there are two groups of priority classes (CA0/CA1 and CA2/CA3) that correspond to different values for the CW_i's.

TABLE I

IEEE 1901 Values for the Contention Windows CW_i and the Initial Values d_i of Deferral Counter DC, for Each Backoff Stage i and Each Priority Class. CA0/CA1 Priorities Are Used for Best-Effort Traffic and CA2/CA3 for Delay-Sensitive Traffic

	Class CA0/CA1		Class CA2/CA3	
backoff stage i	CW_i	d_i	CW_i	d_i
0	8	0	8	0
1	16	1	16	1
2	32	3	16	3
3	64	15	32	15

The main difference between 1901 and 802.11 is that a 1901 station might enter the next backoff stage even if it did not attempt a transmission. This is regulated by the deferral counter DC, which works as follows. When the station enters backoff stage i, DC is set at *an initial DC value* d_i, where d_i is given in Table I for each backoff stage i. After having sensed the medium busy, a station decreases DC by 1 (in addition to BC). If the medium is sensed busy and $DC = 0$, then the station jumps to the next backoff stage (or re-enters the last backoff stage, if it is already at this stage) and re-draws BC *without attempting a transmission*.

The deferral counter was introduced in 1901, so that 1901 can employ small contention window values – which provide good performance for a small number of stations – while avoiding collisions, thus maintaining good performance for a large number of stations. In particular, to reduce collisions, 1901 stations redraw their backoff counter when they sense a number of transmissions before their backoff counter expires; in this way, they react to a high load in the network without the need of a collision, in contrast to 802.11 that only reacts to collisions.

Although the above mechanism achieves its goal, i.e., providing good performance in terms of throughput, it might lead to short-term unfairness: When a station gets hold of the channel and uses a small contention window, it is likely to transmit several frames and thus trigger the deferral counter mechanism of the other stations, which further increase their contention windows and hence reduce even more their probability of accessing the channel. Such a coupling effect penalizes the accuracy of existing models that assume that the backoff processes of different stations are independent.

III. Related Work

The backoff process of 802.11 can be considered as a version of 1901 where the deferral counter DC never reaches 0 (i.e., $d_i = \infty$, for all i). Hence, we first review relevant studies on 802.11 and then we present the existing work on 1901.

A. Analyses of IEEE 802.11

Most work modeling 802.11 performance relies on the decoupling assumption, initially proposed by Bianchi in [5]. Bianchi proposes a model for single contention domains, using a discrete-time Markov chain. Under the decoupling assumption, the collision probability experienced by all stations is

time-invariant and can be found via a fixed-point equation that depends on the parameters of the protocol. Kumar *et al.* [9] examine the backoff process of 802.11 using the same assumptions and renewal theory. The authors also extract a fixed-point equation for the collision probability. The decoupling assumption has later been examined in [10] and [11] (analytically and experimentally) and found to be valid for 802.11.

Sharma *et al.* [12] study 802.11 without the decoupling assumption. They analyze an m-dimensional chain (m being the number of backoff stages) that describes the number of stations at each backoff stage. *Drift equations* capture the expected change of the number of stations at each backoff stage between two consecutive time slots, and their equilibrium point yields the average number of stations at each backoff stage in steady state. Similarly to [12], we also use drift equations to obtain an accurate model for 1901.

B. Analyses of IEEE 1901 Under the Decoupling Assumption

There are a few works analyzing the backoff mechanism of 1901 that rely on the decoupling assumption. First, Chung et al. [6] introduce a model using a discrete-time Markov chain similar to Bianchi's model for 802.11 [5]. The additional state required to capture the effect of the deferral counter DC significantly increases the complexity of the Markov chain.

Our works of [7] and [13] propose a simplification to the model of [6], reducing the Markov chain to a single fixed-point equation; by applying a similar theoretical technique to [9], these papers also prove that this fixed-point equation admits a unique solution. Being less accurate but simpler than the model introduced here, the model of [13] enables us to optimize the performance of the protocol towards high throughput.

Cano and Malone [8] provide a simplification of the analysis of [6] for computing the delay under unsaturated traffic scenarios. They also evaluate the implications of the assumption made in [6] that the buffer occupancy probability is independent of the backoff stage at which the transmission takes place.

IV. Analysis

In this section, we introduce our model for the 1901 CSMA/CA protocol. Our analysis relies on the following network assumptions (all of them widely used [5]–[13]):

- There is a single contention domain with N stations.
- All stations are saturated (always have a packet to send).
- There is no packet loss or errors due to the physical layer, and transmission failures are only due to collisions.
- The stations have an infinite retry limit; that is, they never discard a packet until it is successfully transmitted.[1]

The 1901 standard introduces four different priority classes (see Section II) and specifies that only the stations belonging to the highest contending priority class run the backoff process.[2] In our analysis, we follow this, and we consider a scenario in which all the contending stations use the same set of parameters (corresponding to the highest priority class).

A. Baseline Model

We model the PLC network as a dynamical system that is described by the expected change in the number of stations at each backoff stage between any two consecutive time slots. In the stationary regime, the expected number of stations at each backoff stage is constant hence, we can compute performance metrics by finding the equilibrium of the dynamical system.

Let us now introduce the variables of our model. Let m be the number of backoff stages and let $n_i, 0 \leq i \leq m-1$ denote the number of stations at backoff stage i. Note that $\sum_{i=0}^{m-1} n_i = N$ and $n_i \in \mathbb{N}$. Let us further denote with τ_i the transmission probability at stage i, i.e., τ_i is the probability that a station at backoff stage i transmits at any given time slot. In addition, for a given station at backoff stage i, we denote with p_i the probability that at least one other station transmits. We also denote with p_e the probability that no station transmits (or equivalently, that the medium is idle). Under the assumption of independence of the transmission attempts, we have $p_e = \prod_{k=0}^{m-1} (1-\tau_k)^{n_k}$, therefore

$$p_i = 1 - \frac{p_e}{1-\tau_i} = 1 - \frac{1}{1-\tau_i} \prod_{k=0}^{m-1} (1-\tau_k)^{n_k}. \qquad (1)$$

Model of a Station: We now model the behavior of a given station at backoff stage i. We assume that the event that some other station transmits in a slot occurs with a constant probability p_i, independent of the station's backoff and deferral counters values.[3] Hence, this corresponds to the probability that a transmission of the given station collides, as well as to the probability that the station senses a slot busy when it does not transmit. The rest of the backoff process of the station is modeled accurately as a function of p_i, drawing the station's backoff counter from a uniform distribution. With this model, we derive the probability that a station transmits and that it moves to the stage $i+1$ due to the deferral counter. These two probabilities are used in our network model presented in the next section.

In 1901, a station with DC originally equal to d_i can change its backoff stage either (i) after attempting a transmission or (ii) due to sensing the medium busy d_i+1 times.[4] To compute the probabilities of events (i) and (ii), we introduce x_k^i as the probability that a station at backoff stage i jumps to backoff stage $i+1$ in k or fewer time slots due to (ii). Note that we can compute x_k^i directly from p_i. Let T be the random variable describing the number of slots among k slots during which the medium is sensed busy. Because a station at backoff stage i senses the medium busy with probability p_i at each time slot, T follows the binomial distribution $\mathrm{Bin}(k, p_i)$. This yields

$$x_k^i = \mathbb{P}(T > d_i) = \sum_{j=d_i+1}^{k} \binom{k}{j} p_i^j (1-p_i)^{k-j}. \qquad (2)$$

[1] Contrary to 802.11, 1901 does not specify a retry limit. However, there is a timeout on the frame transmission that is vendor specific. For instance, for the HomePlug AV devices tested in Section V, the timeout for CA1 priority frames is 2.5 s, which is very large compared to the maximum frame duration (2.5 ms [4]). Therefore, the infinite retry limit assumption is reasonable.

[2] In practice, the contending priority class is decided during a so-called *priority resolution phase*, using a simple system of busy tones.

[3] With this assumption, we are neglecting the coupling between the deferral counter decrements of different stations. Note, however, that this does not couple the actual transmissions, as these follow a separate random process; as a result, the coupling due to the deferral counter is somehow diluted.

[4] A major difference between 1901 and 802.11 is that, contrary to 1901, a station using 802.11 can only adapt its backoff because of (i), not of (ii).

Let us denote by bc_i the expected number of time slots spent by a station at backoff stage i. Now, recall that when entering stage i, the stations draw a backoff counter BC uniformly at random in $\{0,\dots,CW_i-1\}$. Let k denote the value of BC. Depending on k, one of the following happens:

- If $k > d_i$, then event (i) occurs with probability $(1-x_k^i)$, in which case the station spends $(k+1)$ slots in stage i (the $(k+1)th$ slot being used for transmission). Now, (ii) occurs with probability x_k^i. More precisely, (ii) occurs at slot j, for $d_i+1 \le j \le k$, with probability $(x_j^i - x_{j-1}^i)$,[5] in which case the station spends j slots in stage i.
- If $k \le d_i$, then (ii) cannot happen. Event (i) takes place with probability 1, which yields that the backoff counter expires and that the station spends $(k+1)$ slots in stage i.

By grouping all the possible cases described above, we have

$$bc_i = \frac{1}{CW_i}\sum_{k=d_i+1}^{CW_i-1}\left[(k+1)(1-x_k^i) + \sum_{j=d_i+1}^{k} j(x_j^i - x_{j-1}^i)\right] + \frac{(d_i+1)(d_i+2)}{2CW_i}. \quad (3)$$

Now, the transmission probability τ_i can be expressed as a function of x_k^i and bc_i, using the renewal-reward theorem, with the number of backoff slots spent in stage i being the renewal sequence and the number of transmission attempts (i.e., 0 or 1) being the reward. The expected number of transmission attempts at stage i can be computed similarly to bc_i. By dividing the expected number of transmission attempts at stage i with the expected time slots spent at stage i, τ_i is given by

$$\tau_i = \frac{\sum_{k=d_i+1}^{CW_i-1}\frac{1}{CW_i}(1-x_k^i) + \frac{d_i+1}{CW_i}}{bc_i}. \quad (4)$$

Similarly, we define β_i as the probability that, at any given slot, a station at stage i moves to the next backoff stage because it has sensed the medium busy d_i+1 times (event (ii)). β_i is given by

$$\beta_i = \frac{\sum_{k=d_i+1}^{CW_i-1}\frac{1}{CW_i}\sum_{j=d_i+1}^{k}(x_j^i - x_{j-1}^i)}{bc_i}. \quad (5)$$

It will be very important in the following to remember that τ_i and β_i are functions of p_i (through x_k^i and bc_i). To simplify the exposition and the analysis of τ_i with respect to p_i, we finally introduce the variable B_i; it is defined as $B_i \doteq 1/\tau_i - 1$. After some computations in (4), we have

$$B_i = \frac{\frac{CW_i(CW_i-1)}{2} - \sum_{k=d_i+1}^{CW_i-1}(CW_i-1-k)x_k^i}{CW_i - \sum_{k=d_i+1}^{CW_i-1}x_k^i}. \quad (6)$$

Our notation is summarized in Table II. We next study the evolution of the expected change in the number of stations at each backoff stage i.

[5]Observe that $(x_j^i - x_{j-1}^i)$ is the difference of two complementary CDFs and denotes the probability that (ii) happens exactly at slot j.

TABLE II
NOTATION LIST RELEVANT TO A STATION AT BACKOFF STAGE i

Notation	Definition (at backoff stage i, $0 \le i \le m-1$)
n_i	Number of stations
p_i	Probability that at least one other station transmits at any slot
p_e	Probability that the medium is idle at any slot (independent of i)
x_k^i	Probability that a station leaves stage i due to sensing the medium busy d_i+1 times during k slots
bc_i	Expected number of backoff slots
τ_i	Probability that a station transmits at any slot
β_i	Probability that, at any slot, a station leaves stage i due to sensing the medium busy d_i+1 times
B_i	$1/\tau_i - 1$
F_i	Expected change in n_i between two consecutive slots
$\bar{n}_i$	Expected number of stations

B. Transient Analysis of the System

Building on the analysis above, we now introduce our model. A key feature is that we do not assume that the stations are decoupled, as the collision probability is allowed to depend on the station's state. To study the system, we use a vector that includes the number of stations at each backoff stage. In particular, let $\mathbf{X}(t) = (X_0(t), X_1(t), \dots, X_{m-1}(t))$ represent the number of stations at each backoff stage $(0,1,\dots,m-1)$ at time slot t. We use the notation $\mathbf{n}(t) = (n_0(t), n_1(t), \dots, n_{m-1}(t))$ to denote a realization of $\mathbf{X}(t)$ at some time slot t.

Network Model (NM): To model the network, we rely on the simplifying assumption that a station transmits, or moves to the next backoff stage upon expiring the deferral counter, with a constant probability (independently of previous time slots). This is necessary as otherwise, we would need to keep track of the backoff and deferral counter values of each station and the model would become intractable. In particular, our assumptions are as follows: (i) a station at backoff stage i attempts a transmission in each time slot with a constant probability $\tau_i(p_i)$; and (ii) a station at backoff stage i moves to backoff stage $i+1$ due to the deferral counter expiration with a constant probability $\beta_i(p_i)$ in each time slot where it does not transmit. Both τ_i and β_i depend on the probability p_i that the station senses a slot busy, which is computed from the transmission probabilities of the other stations following (1).

With the above assumptions, $\mathbf{X}(t)$ is a Markov chain. The transition probabilities τ_i and β_i depend on the state vector $\mathbf{n}(t)$ and they can be computed from (1), (4) and (5); hereafter, to simplify notation, we drop the input variable t from $p_i(t)$, $\tau_i(t)$, $\beta_i(t)$, and $\mathbf{n}(t)$ as the equations are expressed for any slot t.

Let now $\mathbf{F}(\mathbf{n}) = \mathbb{E}[\mathbf{X}(t+1) - \mathbf{X}(t) | \mathbf{X}(t) = \mathbf{n}]$ be the expected change in $\mathbf{X}(t)$ over one time slot, given that the system is at state $\mathbf{n}$. Function $\mathbf{F}(\cdot)$ is called the *drift* of the system, and is given by

$$F_i(\mathbf{n}) = \begin{cases} \sum_{k=1}^{m-1} n_k\tau_k(1-p_k) - n_0\tau_0 p_0 - n_0\beta_0, & i=0 \\ n_{i-1}(\tau_{i-1}p_{i-1} + \beta_{i-1}) - n_i(\tau_i+\beta_i), & 0<i<m-1 \\ n_{m-2}(\tau_{m-2}p_{m-2} + \beta_{m-2}) - n_{m-1}\tau_{m-1}(1-p_{m-1}), & i=m-1. \end{cases} \quad \text{(DRIFT)}$$

(DRIFT) is obtained by balancing, for every backoff stage, the average number of stations that enter and leave this backoff

stage. In particular, n_0 increases by 1 only when some station transmits successfully. Since such a station could be in any of the other backoff stages and there are n_k stations in stage k, this occurs with probability $\sum_{k=1}^{m-1} n_k \tau_k (1-p_k)$. Similarly, n_0 decreases when some stations at stage 0 are either involved in a collision (which occurs with probability $n_0 \tau_0 p_0$), or do not transmit and sense the medium busy d_0+1 times (which occurs with probability $n_0 \beta_0$). The decrease of n_0 in both cases is 1, thus the expected decrease is equal to the sum of the two probabilities. The resulting drift F_0 is computed by adding all these (positive and negative) expected changes in n_0.

Similarly, $F_i,\ 0 < i < m-1$ is computed by observing that in these backoff stages, n_i decreases if and only if some stations at stage i sense the medium busy or transmit. n_i increases if and only if some stations at stage $i-1$ sense the medium busy or transmit and collide. Finally, n_{m-1} increases after some stations at stage $m-2$ experience a collision or sense the medium busy $d_{m-2}+1$ times. It decreases only after a successful transmission at stage $m-1$.

The evolution of the expected number of stations $\bar{\mathbf{n}}(t) \doteq \mathbb{E}[\mathbf{X}(t)]$ is described by the m-dimensional dynamical system

$$\bar{\mathbf{n}}(t+1) = \bar{\mathbf{n}}(t) + \mathbf{F}(\bar{\mathbf{n}}(t)), \tag{7}$$

where $\mathbf{F}(\bar{\mathbf{n}}(t))$ is given by (DRIFT).

Our model relies on the key insight that the stochastic system $\mathbf{X}(t)$ stays close to the typical state given by the equilibrium of (7), and accurate estimates of various metrics such as throughput can be obtained by assuming that the system is in this typical state at all times. However, in reality the stochastic system might stay in other states with a certain probability. In the following, we evaluate the accuracy of approximating our random system by a deterministic model given by (7).

C. Accuracy of the Deterministic Model Approximation

It is intuitive that the approximation becomes more accurate as the number of stations in the system grows: If the number of stations at each backoff stage is very large, the behavior of the stochastic system is expected to be close to the deterministic one given by (7) due to the law of large numbers. This has been proven for 802.11 in [10], [12], and [14]: By analyzing a properly scaled version of the stochastic system, these papers show that the 802.11 stochastic system converges to the deterministic model as the number of stations grows to ∞. In the following, we show the same result for 1901.

As in all the previous analyses of 802.11 [10], [12], [14], we consider a scaled version of our system, $\mathbf{Y^N}(\mathcal{T})$, where time is accelerated by a factor of N while the transition probabilities are scaled down by the same factor, i.e., $\mathbf{Y^N}(t/N) = \mathbf{X}(t)/N$ (this factor N being equal to the number of stations):

- By scaling time, the evolution of time slots is accelerated by N, such that a variable at time t before this operation is translated into the scaled one at time $\mathcal{T} = t/N$.
- By scaling the transition probabilities, the evolution of each node is slowed down by a N.

With this scaling, the expected change of the state of the system between two consecutive time-slots is order of $1/N$, which tends to zero as $N \to \infty$. By accelerating the evolution of time-slots by N, the change of the system over time remains in the same order of magnitude as the original system.

Following this reasoning, to scale down the transition probabilities we let the probability that a station attempts a transmission at backoff stage i be $\tau_i(p_i)/N$, and the probability that it jumps to the next backoff stage due to the expiration of the deferral counter be $\beta_i(p_i)/N$. We further set $y_i(\mathcal{T})$ equal to the fraction of stations at backoff stage i, i.e., $y_i(\mathcal{T}) = n_i(\mathcal{T})/N$. By substituting in (DRIFT) the transition probabilities by the scaled ones, t by $N\mathcal{T}$ and $n_i(\mathcal{T})$ by $N y_i(\mathcal{T})$, we obtain the following deterministic (asymptotic) system as $N \to \infty$:

$$\frac{dy_i}{d\mathcal{T}} = \begin{cases} \sum_{k=1}^{m-1} y_k \tau_k(\rho)(1-\rho) \\ \qquad - y_0(\tau_0(\rho)\rho + \beta_0(\rho)), & i = 0 \\ y_{i-1}(\tau_{i-1}(\rho)\rho + \beta_{i-1}(\rho)) - y_i(\tau_i(\rho) + \beta_i(\rho)), \\ & 0 < i < m-1 \\ y_{m-2}(\tau_{m-2}(\rho)\rho + \beta_{i-1}(\rho)) - y_{m-1}\tau_{m-1}(\rho)(1-\rho), \\ & i = m-1, \end{cases} \tag{ODE}$$

where the collision probability of a station at stage i is given by $\rho = \lim_{N\to\infty} 1 - \frac{\prod_{k=0}^{m-1}(1-\tau_k(\rho)/N)^{n_k}}{1-\tau_i(\rho)/N} = 1 - e^{-\sum_{k=0}^{m-1} y_k \tau_k(\rho)}$.

The following theorem shows that the stochastic system under study converges to the deterministic model given above as $N \to \infty$, which confirms that the proposed analysis becomes very accurate as the number of stations grows large.

Theorem 1: As $N \to \infty$, the scaled random system $\mathbf{Y^N}(\mathcal{T})$ converges to the deterministic process $\mathbf{y}(\mathcal{T})$ given by (ODE).

Proof: The proof follows from [15], which establishes the convergence of $\mathbf{Y^N}(\mathcal{T})$ to $\mathbf{y}(\mathcal{T})$ when the following conditions are satisfied[6]: (i) there exists a 'vanishing intensity' $\epsilon(N)$ such that $\lim_{N\to\infty} \mathbf{F}(\mathbf{n}, N)/\epsilon(N)$ exists, $\mathbf{F}(\mathbf{n}, N)$ being the drift function $\mathbf{F}(\mathbf{n})$ of the scaled system for a given N; (ii) $\mathbb{E}[W_N^2] < c_1 N^2 \epsilon(N)^2$, where W_N is an upper bound on the number of stations that do a transition in a time-slot in the scaled system and c_1 is a positive constant; and (iii) $\mathbf{F}(\mathbf{n}, N)$ is a smooth function of $\mathbf{n}$ and N (i.e., it has continuous derivatives everywhere including at the boundary).

By taking the 'vanishing intensity' $\epsilon(N) = 1/N$, it follows that $\lim_{N\to\infty} \mathbf{F}(\mathbf{n}, N)/\epsilon(N)$ can be expressed as a function of $\tau_i(\rho)$ and $\beta_i(\rho)$, and hence condition (i) is satisfied.

To verify condition (ii), we let $\alpha = \max_{i,p_i}(\tau_i(1-p_i), \tau_i p_i + \beta_i)$. Note that $\alpha < 1$.[7] Then, the probability that a station changes its state is upper bounded by α/N, and the number of stations that change their state is stochastically upper bounded by a random variable W_N that follows the binomial distribution $\text{Bin}(N, \alpha/N)$.[8] Thus, we have $\mathbb{E}[W_N^2] = \mathbb{E}[W_N]^2 + \text{Var}[W_N] < \alpha^2 + \alpha$, and condition (ii) is satisfied.

Finally, both τ_i and β_i are smooth functions of p_i which in turn is a smooth function of the n_i's, and hence, the transition

[6]Note that assumptions H1 and H4 of [15] do not apply to our system, since the system does not have the so-called 'common resource'.

[7]We have $\alpha < 1$, given that $\tau_i(1-p_i) < 1$ and $\tau_i p_i + \beta_i < 1$ (the latter follows from $\tau_i + \beta_i = 1/bc_i < 1$).

[8]Note that, under our network model, a station changes its state independently of the transitions of the other stations.

probabilities are smooth functions of $\mathbf{n}$. Additionally, the transition probabilities are also smooth functions of N. This also holds for the boundaries of the transition probabilities, including $N \to \infty$. Therefore, condition (iii) is satisfied. ■

D. Steady-State Analysis of the System

We next study the the system under steady state. To obtain the average number of stations at each backoff stage in steady state, we compute the equilibrium point(s) of system (7) corresponding to the stationary regime. To compute the equilibrium point(s) of (7), we impose $\mathbf{F}(\bar{\mathbf{n}}) = \mathbf{0}$, which yields

$$\bar{n}_i = \left(\frac{\tau_{i-1}p_{i-1} + \beta_{i-1}}{\tau_i + \beta_i}\right)\bar{n}_{i-1}, \quad 1 \le i \le m-2,$$
$$\bar{n}_{m-1} = \left(\frac{\tau_{m-2}p_{m-2} + \beta_{m-2}}{\tau_{m-1}(1-p_{m-1})}\right)\bar{n}_{m-2}.$$

Let us define

$$K_0 \doteq 1, \quad K_i \doteq \frac{\tau_{i-1}p_{i-1} + \beta_{i-1}}{\tau_i + \beta_i}, \quad 1 \le i \le m-2,$$
$$K_{m-1} \doteq \frac{\tau_{m-2}p_{m-2} + \beta_{m-2}}{\tau_{m-1}(1-p_{m-1})}. \tag{8}$$

Since $\sum_{i=0}^{m-1} \bar{n}_i = N$, the equilibrium $\hat{\mathbf{n}}$ of (7) is given by

$$\hat{n}_i = \frac{N\prod_{j=0}^{i} K_j}{\sum_{k=0}^{m-1}\prod_{j=0}^{k} K_j}, \quad 0 \le i \le m-1. \tag{EQ}$$

Recall that τ_i and β_i are functions of p_i, given by (4) and (5). Thus, the $\hat{n}_i$'s in (EQ) are also functions of p_i, $0 \le i \le m-1$. From the above, substituting (EQ) in (1) yields a system of m equations with m unknowns p_i for $0 \le i \le m-1$.

After solving the equations for finding the steady-state number of nodes $\hat{n}_0, \ldots, \hat{n}_{m-1}$ at each backoff stage, we can compute the throughput of the network as follows. The probability that a slot is idle is p_e. The probability of a successful transmission of a station at stage i is $\tau_i(1-p_i)$. Therefore, the probability p_s that a slot contains a successful transmission is given by $p_s = \sum_{i=0}^{m-1} \hat{n}_i\tau_i(1-p_i)$, assuming that $\mathbf{n}$ remains in a neighborhood of the equilibrium point $\hat{\mathbf{n}}$. Let p_c denote the probability that a slot contains a collision. We have $p_c = 1 - p_e - p_s$. We now have enough information to compute the normalized throughput S of the network as

$$S = \frac{p_s D}{p_s T_s + p_c T_c + p_e \sigma}, \tag{9}$$

where D is the frame duration, T_s is the duration of a successful transmission, T_c is the duration of a collision, and σ is the time slot duration. In Section V, we evaluate the stationary regime of the system, and show that our model is very accurate for a wide range of configurations.

E. Uniqueness of the Equilibrium Point

In this subsection we prove that, as long as the configuration of CW_i's and d_i's is chosen such that the sequence τ_i is decreasing with i for any n_i distribution, then the equilibrium point given by (EQ) is unique. We argue that such a condition should be met by any sensible configuration of CW_i's and d_i's. The argument is as follows. Jumping to the next backoff stage is an indication of high contention, either because of a collision or a sequence of busy slots. Therefore, in this case τ_i should decrease with i, and the high contention should be dissolved by reducing the aggressiveness of the sources. Note that similar studies for the 802.11 MAC protocol [9], [10] require the same sufficient condition (i.e., τ_i decreasing with i) for the model to admit a unique solution. To simplify the exposition, we define this condition as follows.

$$\tau_i > \tau_{i+1}, \quad 0 \le i \le m-2. \tag{COND}$$

We now prove, in Theorem 2, that if (COND) is satisfied, the equilibrium point given by (EQ) is unique.

Theorem 2: The system of equations formed by (EQ) and (1) for $0 \le i \le m-1$ has a unique solution if (COND) is satisfied.

Proof: Recall that $p_e = \prod_{k=0}^{m-1}(1-\tau_k)^{\hat{n}_k}$. For any value of p_e, τ_i can be computed from the fixed-point equation that results from combining (1) (i.e., $p_i = 1 - p_e/(1-\tau_i)$) with (4), where (4) is expressed as a function of p_i through (2). Hence, τ_i can be computed as a function of p_e, and so can p_i, and β_i. Now, $\hat{n}_i$ can also be computed as a function of p_e using (EQ). Let $\Phi(p_e) \doteq \prod_{k=0}^{m-1}(1-\tau_k(p_e))^{\hat{n}_k(p_e)}$. Then, a solution of (EQ) has to satisfy the following equation:

$$p_e = \Phi(p_e). \tag{10}$$

It can be seen that (10) has at least one fixed-point. $\Phi(p_e)$ is defined in $[0, 1-\tau_{max}]$, where $\tau_{max} := 2/(CW_0+1)$ is the maximum transmission probability at stage 0. Observe that $\Phi(0) > 0$ and $\Phi(1-\tau_{max}) < 1-\tau_{max}$ thus, by the intermediate value theorem, $\Phi(p_e)$ has at least one fixed-point in $[0, 1-\tau_{max}]$. We now show that (10) has only one fixed-point. To this end, we show that $\Phi(p_e)$ is monotonically decreasing with p_e. The derivative of $\Phi(p_e)$ can be written as

$$\frac{d\Phi(p_e)}{dp_e} = \sum_{j=0}^{m-1}\left(\frac{\partial\Phi}{\partial p_j}\frac{dp_j}{dp_e} + \frac{\partial\Phi}{\partial\beta_j}\frac{d\beta_j}{dp_e} + \frac{\partial\Phi}{\partial\tau_j}\frac{d\tau_j}{dp_e}\right). \tag{11}$$

We now examine separately each of the partial derivative products of (11) with respect to p_j, β_j and τ_j. To prove the theorem, we rely on our analysis in the Appendix. First, Lemmas 2 and 3 imply respectively that $dp_j/d\tau_j < 0$ and $d\tau_j/dp_e < 0$. Because $dp_j/dp_e = (dp_j/d\tau_j)\cdot(d\tau_j/dp_e)$, we have $dp_j/dp_e < 0$. Also, from Lemma 5, we have $\partial\Phi/\partial p_j > 0$. Thus, the first product of partial derivatives in (11) is negative for all j. Second, from Lemma 4, we have $\partial\Phi/\partial\beta_j \ge 0$. Now, Corollary 1 states that $d\beta_j/dp_j > 0$ and we have shown above that $dp_j/dp_e < 0$. Hence, we have $d\beta_j/dp_e < 0$ thus, the second product of partial derivatives in (11) is also negative. Third, from Lemma 6 we have $\partial\Phi/\partial\tau_j < 0$, and from Lemma 3 we have $d\tau_j/dp_e > 0$. We have shown that all the partial derivative products of (11) are negative, so $\Phi(p_e)$ is monotonically decreasing with p_e.

Since (11) is strictly negative and (10) admits at least one fixed-point, there exists a unique value for p_e that solves (10). Computing the corresponding value for p_i by (1), we have a solution to (EQ). The uniqueness of the solution then follows from the fact that all relationships between τ_i, β_i, p_i and p_e

are bijective, and any solution must satisfy (10), which (as we have shown) has only one solution. ■

We next provide some configuration guidelines for (CW_i, d_i) that ensure that (COND) is satisfied. In Section V, we discuss a counterexample of a configuration that does not satisfy (COND) and does not yield a unique solution to the system of equations formed by (EQ) and (1).

F. Protocol Configurations Satisfying (COND)

Before showing in Theorem 3 that (COND) is satisfied for a wide range of configurations, we prove a useful lemma. Note that compared to 802.11, where τ_i is a function of only CW_i, the analysis here is substantially more challenging, because τ_i is a function of CW_i, d_i, and p_i.

We have to investigate the relationship between τ_i and τ_{i+1}. Recall that these two transmission probabilities are functions of two different collision probabilities p_i and p_{i+1}, respectively, which makes the analysis challenging. Assume that the collision probability is the same for two successive backoff stages i and $i+1$, and is equal to p_i. Under this hypothesis, in Lemma 1, we show that if $\tau_i(p_i) > \tau_{i+1}(p_i)$, $\forall p_i \in [0,1]$, then $\tau_i(p_i) > \tau_{i+1}(p_{i+1})$, for any pair p_i, p_{i+1} that satisfies (1). In Theorem 3, we provide some sufficient conditions to guarantee that $\tau_i(p_i) > \tau_{i+1}(p_i)$ is satisfied for all $p_i \in [0,1]$ and $0 \leq i < m-1$; from Lemma 1, this implies that (COND) is satisfied.

Lemma 1: Let p_i^s be a value of the collision probability at stage i. Then, if $\tau_i(p_i^s) > \tau_{i+1}(p_i^s)$ for all $p_i^s \in [0,1]$, we have $\tau_i(p_i) > \tau_{i+1}(p_{i+1})$ for any n_i distribution.

Proof: The proof goes by contradiction. Let us assume that there exists a solution $\mathbf{n^s}$, such that the corresponding values of τ_i^s, p_i^s, τ_{i+1}^s and p_{i+1}^s, p_e^s satisfy $\tau_i^s(p_i^s) < \tau_{i+1}^s(p_{i+1}^s)$ and (consequently) $p_i^s > p_{i+1}^s$. Note that, for any n_i distribution, p_i and p_{i+1} satisfy (1). Due to (1), we have

$$\frac{1-p_i^s}{1-p_{i+1}^s} = \frac{1-\tau_{i+1}^s}{1-\tau_i^s}. \tag{12}$$

Let us fix τ_i and p_i to the values given by the solution described above, and vary p_{i+1} by choosing different values of γ, defined as $1-p_{i+1} \doteq \gamma(1-p_i^s)$. For each γ, we first compute τ_{i+1} that corresponds to this p_{i+1}, and then we compute the expression $(1-\tau_i^s)/(1-\tau_{i+1})$ that results from this τ_{i+1} and the (fixed) τ_i^s value. Then, if such a solution s exists, there must be some value of $\gamma \geq 1$ for which

$$f(\gamma) \doteq \frac{1-\tau_i^s}{1-\tau_{i+1}(\gamma)} = \gamma,$$

because of (12) and the definition of γ. Next, we show that such a γ does not exist, which contradicts our initial assumption.

By hypothesis, for $\gamma = 1$ we have $p_{i+1} = p_i^s$, so $\tau_i(p_i^s) > \tau_{i+1}(p_i^s)$, and $f(1) < 1$. A sufficient condition to ensure that there exists no $\gamma > 1$ value for which $f(\gamma) = \gamma$ is that the derivative of $f(\gamma)$, i.e. $df(\gamma)/d\gamma$, does not exceed 1 in the region $\gamma \geq 1$. To prove this, we proceed as follows.

$$\begin{aligned}
\frac{df(\gamma)}{d\gamma} &= \frac{1-\tau_i^s}{(1-\tau_{i+1})^2}\frac{d\tau_{i+1}}{d\gamma} = \frac{1-\tau_i^s}{(1-\tau_{i+1})^2}\frac{d\tau_{i+1}}{dp_{i+1}}\frac{dp_{i+1}}{d\gamma} \\
&= -\frac{(1-\tau_i^s)(1-p_i^s)}{(1-\tau_{i+1})^2}\frac{d\tau_{i+1}}{dB_{i+1}}\frac{dB_{i+1}}{dp_{i+1}} \\
&= \frac{(1-\tau_i^s)(1-p_i^s)\tau_{i+1}^2}{(1-\tau_{i+1})^2}\frac{dB_{i+1}}{dp_{i+1}} \\
&\overset{\gamma\geq 1}{\leq} \frac{(1-p_{i+1})\tau_{i+1}^2}{(1-\tau_{i+1})^2}\frac{dB_{i+1}}{dp_{i+1}} = \frac{(1-p_{i+1})}{B_{i+1}^2}\frac{dB_{i+1}}{dp_{i+1}}.
\end{aligned}$$

From the above, it is sufficient to prove $dB_{i+1}/dp_{i+1} \leq B_{i+1}^2/(1-p_{i+1})$. This is shown in Corollary 2 in the Appendix for $p_{i+1} \in [0,1)$. For $p_{i+1} = 1$, we also have $p_i = 1$ by (1). Thus, a solution s cannot exist and $\tau_i(p_i) > \tau_{i+1}(p_{i+1})$. ■

The following theorem provides some sufficient conditions on the (CW_i, d_i) configurations that ensure that (COND) holds. Notably, Lemma 1 can be employed to show that (COND) holds for more configurations than the ones covered by the theorem; indeed, it is sufficient to show that the configuration satisfies the hypothesis of the Lemma 1 for all $0 \leq i \leq m-2$.

Theorem 3: (COND) holds if the following condition is satisfied for $0 \leq i \leq m-2$

$$CW_{i+1} > \begin{cases} CW_i, & \text{if } d_{i+1} = d_i \\ 2CW_i - d_i - 1, & \text{otherwise.} \end{cases} \tag{13}$$

Proof: We analyze two cases: 1) $d_{i+1} = d_i$; 2) $d_{i+1} \neq d_i$.

1) We start for the case $d_{i+1} = d_i$. By using Lemma 1, we need only to prove that $\tau_{i+1}(p_i) < \tau_i(p_i)$. If this is satisfied for $CW_{i+1} = CW_i + 1$, by using induction it is easy to see that it holds for any $CW_{i+1} > CW_i$. Now, as $\tau_i = 1/(B_i+1)$, it is sufficient to show that $B_{i+1} > B_i$ when $CW_{i+1} = CW_i + 1$.

Due to space constraints, we only provide a sketch of the proof. First, we compute the difference $B_{i+1} - B_i$ by using (6). Recall that $x_k^i = x_k^{i+1}$ for all $d_i + 1 \leq k \leq CW_i - 1$, so we rearrange the terms that cancel out. Next, we rely on two inequalities: First, we use $x_{CW_i}^i \geq x_k^i$, $d_i + 1 \leq k \leq CW_i - 1$ (with equality at $p_i = 0, 1$), so $\sum_{j=d_i+1}^{CW_i-1} x_j^i \leq (CW_i - d_i - 1)x_{CW_i}^i \leq CW_i x_{CW_i}^i$. Second, we use $x_j^i \leq 1$.

2) We now look at the case $d_{i+1} \neq d_i$. The result for this case follows from Lemma 2 in the Appendix. Using this, the minimum value of B_i is $B_i^{min} \doteq (CW_i - 1)/2$ at $p_i = 0$, and its maximum value is $B_i^{max} \doteq CW_i - d_i/2 - 1$ at $p_i = 1$. Setting $CW_{i+1} > 2CW_i - d_i - 1$ yields $B_{i+1}^{min} > B_i^{max}$. Hence, $B_{i+1} > B_i$ for all $p_i \in [0,1]$, $p_{i+1} \in [0,1]$. ■

Observe that, from Table I, the above constraints on CW_i and d_i are compliant with the standard, except for the class CA2/CA3 at backoff stage $i = 1$. The results obtained in this paper suggest that it might be worth to revisit the configuration of this priority class; indeed, for the proposed configuration of CA2/CA3 we have $\tau_2 > \tau_1$ and (COND) does not hold.

We next discuss whether (COND) is sufficient for the global asymptotic stability of (EQ).

G. Global Asymptotic Stability and Convergence

In addition to showing that our system has only one equilibrium point, it is also interesting to show that it converges

to this equilibrium point from all possible initial states. In the following, we study the global stability of the system to assess its convergence to the equilibrium. We first study analytically the system (ODE) given in Section IV-C, and present two theorems that guarantee that it is globally asymptotically stable for $m = 2$ and $m = 3$, respectively. Then, we provide additional numerical results that show that the system given by (7) converges for a wide range of values of m as well as of the other system parameters.

Theorem 4: If (COND) is satisfied, the system (ODE) is globally asymptotically stable for $m = 2$.

Proof: Let us consider the Lyapunov function $L(\mathbf{y}) = (y_0(t)-\hat{y}_0)^2+(y_1(t)-\hat{y}_1)^2$, where $\{\hat{y}_0, \hat{y}_1\}$ is the equilibrium point of (ODE). Let $\gamma(t) \doteq \tau_0 y_0(t) + \tau_1 y_1(t)$ (observe that $\rho = 1 - e^{-\gamma}$). We start by proving that, if at some time t we have $y_0(t) > \hat{y}_0$, this implies $\gamma(t) > \hat{\gamma}$. This can be seen by contradiction. Let us assume $\gamma(t) < \hat{\gamma}$. Given $y_0(t) > \hat{y}_0$, it holds $y_1(t) < \hat{y}_1$ from $y_0(t) + y_1(t) = 1$. Then, from $\gamma = -\ln(1-\rho)$ and Lemma 2 in the Appendix we have $\tau_0 > \hat{\tau}_0$ and $\tau_1 > \hat{\tau}_1$. Thus, $\gamma = \tau_0 y_0(t) + \tau_1 y_1(t) > \hat{\tau}_0 y_0(t) + \hat{\tau}_1 y_1(t) > \hat{\tau}_0 \hat{y}_0(t) + \hat{\tau}_1 \hat{y}_1(t) = \hat{\gamma}$, since $\hat{\tau}_0 > \hat{\tau}_1$ holds from (COND). This contradicts the initial assumption.

Given $\gamma(t) > \hat{\gamma}$, we have $\tau_0(1 - e^{-\gamma}) + \beta_0 > \hat{\tau}_0(1 - e^{-\hat{\gamma}}) + \hat{\beta}_0$. This can be seen as follows. By employing a similar reasoning to Corollary 1, we have $\partial(\tau_0+\beta_0)/\partial\gamma > 0$. We also have $-\partial(\tau_0 e^{-\gamma})/\partial\gamma > 0$ from Lemma 2. Then, adding both expressions we obtain $\partial(\tau_0(1 - e^{-\gamma}) + \beta_0)/\partial\gamma > 0$. Given $\gamma(t) > \hat{\gamma}$, we also have $\tau_1 e^{-\gamma} < \hat{\tau}_1 e^{-\hat{\gamma}}$. Thus,

$$\begin{aligned}\frac{dy_0(t)}{dt} &= -y_0(\tau_0(1 - e^{-\gamma}) + \beta_0) + y_1\tau_1 e^{-\gamma} \\ &< -y_0(\hat{\tau}_0(1 - e^{-\hat{\gamma}}) + \hat{\beta}_0) + y_1\hat{\tau}_1 e^{-\hat{\gamma}} \\ &< -\hat{y}_0(\hat{\tau}_0(1 - e^{-\hat{\gamma}}) + \hat{\beta}_0) + \hat{y}_1\hat{\tau}_1 e^{-\hat{\gamma}} = 0.\end{aligned}$$

Since $dy_0(t)/dt + dy_1(t)/dt = 0$, this in turn implies $dy_1(t)/dt > 0$. Putting all this together yields

$$\frac{dL(\mathbf{y})}{dt} = 2(y_0(t) - \hat{y}_0)\frac{dy_0(t)}{dt} + 2(y_1(t) - \hat{y}_1)\frac{dy_1(t)}{dt} < 0.$$

Similarly, it can be seen that if $y_0(t) < \hat{y}_0$, then $dy_0(t)/dt > 0$ and $dy_1(t)/dt < 0$. We have $dL(\mathbf{y})/dt < 0$ also in this case. Therefore, the system is globally asymptotically stable. ∎

Theorem 5: If (COND) is satisfied, the system (ODE) is globally asymptotically stable for $m = 3$.

Proof: See the Appendix. ∎

In order to show the convergence of the system for other values of m, we have conducted a comprehensive numerical study for the dynamical system given by (7), comprising all the values of the parameters CW_i, m and d_i that satisfy (COND) within the ranges $CW_i = \{8, 16, 32, 64\}$, $m = \{3, 4, 5, 6\}$ and $d_i = \{0, 1, 2, 3, 4, 5, 6, 7, 8, 9, 10, 15, 20, 25, 30\}$. For each configuration, we have randomly chosen 100 different initial points and evaluated the trajectory of the system until it converges (with an error of 10^{-8}). In total, around 10^6 tests of convergence have been conducted, and in every test, the system converges to the equilibrium given by (EQ). All these (numerical and theoretical) results provide very strong evidence of the convergence of the system.

TABLE III
SIMULATION PARAMETERS

Parameter	Duration (μs)
Slot σ, Priority slot PRS	35.84
$CIFS$	100.00
$RIFS$	140.00
Preamble P, ACK	110.48
Frame duration D	2500.00
$EIFS$	2920.64

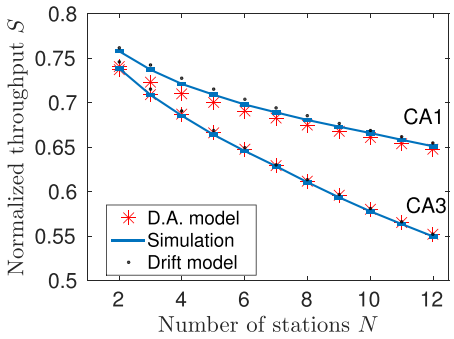

Fig. 2. Throughput obtained by simulation, with our model, and the models based on the decoupling assumption (D.A.), for the default configurations of 1901 given in Table I.

V. PERFORMANCE EVALUATION

In this section, we evaluate the performance of 1901 under different configurations and scenarios as follows. We first compare the accuracy of our model against a model that relies on the decoupling assumption, called "D.A." model [7]. Furthermore, we evaluate other aspects of our model, such as the performance of the configurations that do not satisfy (COND) and the accuracy of our model in the transient regime.

We conduct simulations for a wide range of configurations (CW_i, d_i), comprising the parameters recommended by the 1901 standard as well as more broad configurations, following the recommendations of [1] and [13]. We consider the following timing parameters. We use the same time slot duration and timing parameters as specified in the standard (see Table III). The PLC frame transmission has a duration D and is preceded by two priority tone slots (PRS), and a preamble (P). It is followed by a response inter-frame space ($RIFS$), the ACK, and finally, the contention inter-frame space ($CIFS$). Thus, a successful transmission has a duration $T_s \doteq 2PRS + P + D + RIFS + ACK + CIFS$. In the case of a collision, the stations set the virtual carrier sense (VCS) timer equal to $EIFS$, where $EIFS$ is the extended inter-frame space used by 1901, and then the channel state is *idle*. Hence, a collision has a duration $T_c \doteq EIFS$. Finally, we assume that all the packets use the same physical rate.[9]

A. Comparison With Decoupling Assumption Model

We first compare our model (which hereafter we refer to as "drift model") with the D.A. model for various configurations and number of stations. In Figure 2, we show the throughput obtained by 1901 with the default parameters for the two priority classes CA1 and CA3 (CA0 and CA2 are equivalent).

[9]We wrote a Matlab simulator that implements the full CSMA/CA mechanism of 1901. The simulator has been validated experimentally [1].

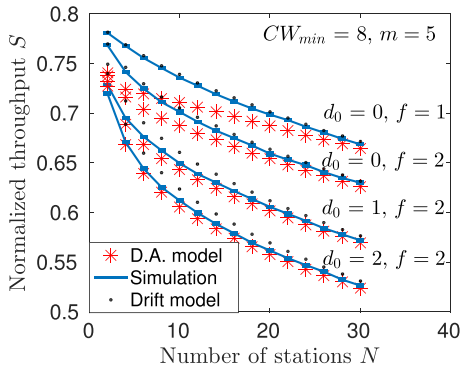

Fig. 3. Throughput obtained by simulation, with the drift model, and the D.A. model for different configurations. The initial values d_i of the deferral counter at each backoff stage are given by $d_i = f^i(d_0 + 1) - 1$.

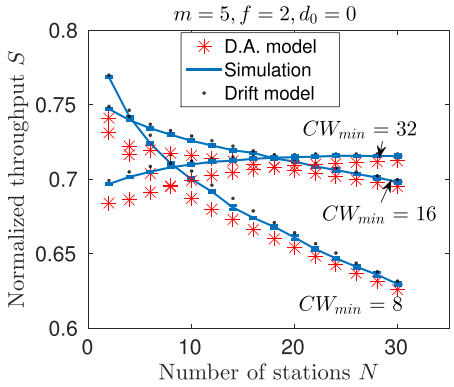

Fig. 4. Throughput obtained by simulation, with the drift model, and the D.A. model for various values of CW_{min}.

We also show the throughput predicted by the two models. The model based on the decoupling assumption is substantially less accurate for CA1 when N is small, because the class CA1 uses larger contention windows, which increases the time spent in backoff and, as a result, the coupling between stations.

We now study the accuracy of the two models in more general settings. To this end, we introduce a factor f, such that at each stage i, the value of d_i is given by $d_i = f^i(d_0 + 1) - 1$. This enables us to define various sequences of values for the d_i's, using only f and d_0. At each stage i, CW_i is given by $CW_i = 2^i CW_{min}$, and there are m backoff stages ($i \in \{0, m-1\}$). In Figure 3, we show the throughput for various such values of d_0 and f, with $CW_{min} = 8$ and $m = 5$. We observe that the D.A. model achieves good accuracy when the d_i's are large, because in these configurations, the deferral counter is less likely to expire, which reduces the coupling among stations. Note that the drift model achieves good accuracy when the d_i's are small, while there is a small deviation for large d_i's; this is due to the assumptions of our network model (NM) of Section IV-B, which are not used by the D.A. model.[10]

Finally, in Figure 4 we show the throughput for different values for CW_{min}. In all cases, the drift model closely follows simulation results, in contrast to the D.A. model.

B. Uniqueness of the Solution and Selected Counterexample

One of the fundamental results of our steady-state analysis is that there is a unique equilibrium for configurations that satisfy (COND). In this subsection we investigate the performance of the system depending on the (non-)unicity of the equilibrium of the dynamical system. To this end, we explore a counterexample of a configuration that does not satisfy (COND) and does not yield a unique equilibrium for the dynamical system (7). An example of such a configuration, which yields 3 equilibrium points for $N = 10$,[11] is the following:

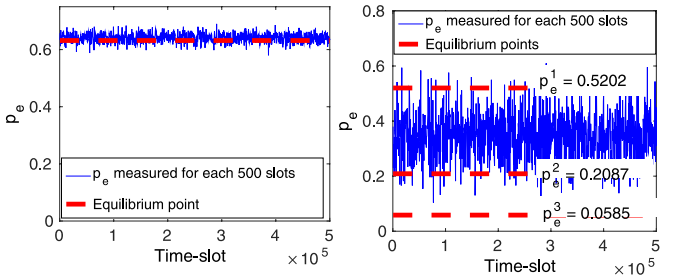

Fig. 5. Simulation of a system with a unique equilibrium point (left, configuration of CA1 class) and with 3 equilibrium points (right, configuration given by (14)). The probability p_e is computed for each 500 slots and is shown for one simulation run (plain black). The values of the equilibrium point(s) are also shown for each system (dashed red). The same behavior was observed for both systems for multiple simulation runs, not shown here.

$$\{CW_i, d_i\} = \begin{cases} \{32, 3\}, & 0 \le i \le 3 \\ \{4, \infty\}, & 4 \le i \le 53 \\ \{64, 3\}, & 54 \le i \le 59. \end{cases} \quad (14)$$

To study this configuration, we compute the instantaneous p_e, i.e, the probability that a time-slot is idle, for every 500 slots in simulation. Figure 5 shows the results for the CA1 class and for the configuration given by (14). We observe that for CA1 class, for which we have a unique equilibrium, the instantaneous p_e is approximately equal to the one given by the equilibrium point of the dynamical system (7). However, for configuration (14) p_e oscillates between two of the equilibrium points and the value of p_e averaged the entire simulation run is not equal to any of the equilibrium points; indeed the average p_e obtained by one simulation run is 0.3478, whereas the values of the equilibrium points of (7) are $(p_e^1, p_e^2, p_e^3) = (0.5202, 0.2087, 0.0585)$.

Our results show that the equilibrium points (EQ) are not sufficient to characterize the performance of the real system when (EQ) are not unique: The real system might oscillate and, as a result, the behavior might not be close to any of the equilibrium points. They also suggest that such configurations should be avoided as they might lead to an unstable thus, undesirable behavior. Indeed, multiple equilibria yield metastable regimes and typically involve severe unfairness or network collapse. For instance, with configuration (14) some stations remain at a state with $CW_i = 4$ for long periods, leading to a very high collision probability and low throughput. The problems resulting from metastable regimes are reported in [19] for 802.11.

[10]The 802.11 model that does not rely on the decoupling assumption [12] has a similar deviation compared to Bianchi's model [5].

[11]These 3 equilibrium points have been obtained by plotting $\Phi(p_e)$ (see the proof of Theorem 2) and computing the fixed-points for which $p_e = \Phi(p_e)$.

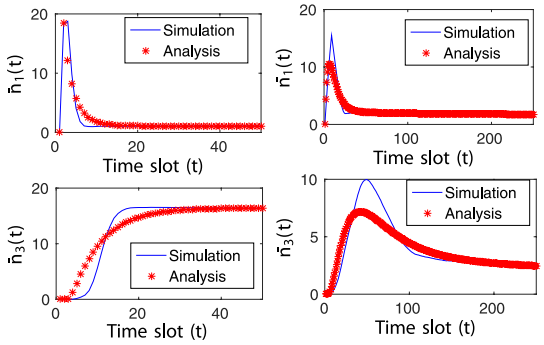

Fig. 6. Convergence to the equilibrium point of the number of stations for backoff stages 1 and 3, for the CA1 class (left) and for a configuration with $d_i \to \infty$ and $CW_i = 2^i CW_0$, $\forall i$, $CW_0 = 8$, $m = 7$, (right). Both the expected values obtained from (7) and the average values obtained from 2000 simulation runs are shown.

C. Accuracy of the Drift Model in the Transient Regime

The above experiments have focused on the accuracy of our steady-state analysis for the stationary regime. In the following, we investigate the accuracy of the analysis for the transient regime. To this end, we consider a system with $N = 20$ stations and two different configurations, and compare the expected number of stations $\bar{\mathbf{n}}(t)$ obtained from (7) and from simulations, as a function of the time slot t, when the initial condition at time slot 0 is $\mathbf{n}(0) = \{20, 0, 0, ..., 0, 0\}$.

We focus on a configuration that follows the 1901 standard, i.e., CA1 class, and on a configuration that follows the 802.11 standard, i.e., the deferral counter does not expire. The results from the experiments described above are shown in Figure 6. We observe that our model works well both in terms of accuracy and of convergence times. As far as accuracy is concerned, there is slightly higher inaccuracy in the transient regime than in the stationary regime, which is due to the assumption on the constant transition probabilities β_i and τ_i.[12] The convergence time to the equilibrium points is also captured by our model with reasonable accuracy. This time is higher for the 802.11 system for two reasons: 1) in the 802.11 system, the stations are allowed to have larger backoff counters and to move into higher backoff stages; 2) in the 1901 system, the stations change their backoff stage with a higher probability than in 802.11 due to the deferral counter.

D. Configuration Guidelines With Respect to (COND)

As discussed in Section IV-E, (COND) is not only a condition for uniqueness, but also a configuration guideline for proper reaction to high contention. Jumping to the next backoff stage is an indication of high contention hence, to dissolve the current contention, the transmission aggressiveness should decrease, that is $\tau_{i+1} < \tau_i$. We now show that configurations where τ_i is increasing with i perform poorly. To confirm this, in the following we run several experiments with different α values, where α is the multiplicative factor of the contention windows between successive backoff stages, i.e., $CW_{i+1} = \alpha CW_i$. Figure 7 presents throughput obtained by simulation and with our model for various values of α, with $CW_i = \lfloor \alpha^{i-1} \cdot 8 \rfloor$, $d_i = \lceil \alpha^{i-1} - 1 \rceil$, $0 \le i \le 4$. Results show that configurations with τ_i increasing, i.e., $\alpha < 1$, yield poor performance. This supports our argument that (COND) should be met to ensure good performance. Theorem 3 provides some configuration guidelines to ensure that (COND) is satisfied.

[12]To confirm that the deviations are due to this assumption, we simulated the Markov chain $\mathbf{X}(t)$ with constant transition probabilities, and verified that the trajectory of $\mathbf{X}(t)$ averaged over 300 runs coincides with the solution of (7).

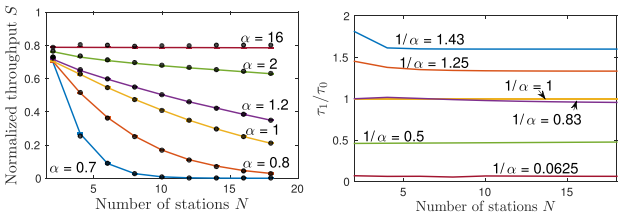

Fig. 7. Performance of 1901 with parameters $CW_i = \lfloor \alpha^{i-1} \cdot 8 \rfloor$, and $d_i = \lceil \alpha^{i-1} - 1 \rceil$ for different values of α. Lines represent throughput obtained by simulation and points show throughput computed by our model (left). We also present the ratio τ_1/τ_0 computed using our model (right).

As it can be seen from the figure, throughput performance improves for large α. However, a closer look at the protocol behavior for different α's reveals that, while large α's provide very good throughput performance, they also suffer from severe unfairness. Indeed, for such configurations only one station grasps the channel, while the others move to higher backoff stages with much larger CW_i values and barely transmit. This shows that throughput considerations are not sufficient to properly evaluate the suitability of a given 1901 configuration, and short-term fairness also needs to be taken into account.

VI. Conclusion

Although the IEEE 1901 CSMA/CA protocol is adopted by the vast majority of PLC devices nowadays, it has received little attention from the research community so far. In this paper, we focus on the performance analysis of this protocol. Our analysis comprises performance in steady-state as well as in the transient regime, and involves both the long-term and the short-term dynamics of 1901. One of the key results of the analysis is the finding that the decoupling assumption, which is commonly adopted for the analysis of MAC protocols such as IEEE 802.11 and 1901, might not hold for 1901. This is due to the coupling that 1901 introduces to the stations contending for the medium. Building on this finding, we have proposed a model that does not rely on the decoupling assumption, and as a result, substantially improves the accuracy of previous analyses. Accuracy is particularly improved for networks with a small number of stations, which is the most frequent scenario in practice. We have shown that our model admits a unique solution for a wide range of configurations.

Appendix

Lemma 2: B_i is an increasing function of p_i, and τ_i is a decreasing function of p_i for any $0 \le i \le m-1$.

Proof: The reader is referred to [1] for the proof of this lemma. ■

Corollary 1: β_i is an increasing function of p_i.

Proof: The reader is referred to [1] for the proof of this corollary. ■

Corollary 2: For any value of i, $dB_i/dp_i < B_i^2/(1-p_i)$ $\forall p_i \in [0,1)$, and $dB_i/dp_i < B_i/p_i$ $\forall p_i \in (0,1]$.

Proof: We start with the first inequality. The derivative dB_i/dp_i can be computed from (6) as

$$\frac{dB_i}{dp_i} = \frac{\sum_{k=d_i+1}^{CW_i-1}(B_i-(CW_i-1-k))\frac{dx_k^i}{dp_i}}{CW_i-\sum_{j=d_i+1}^{CW_i-1}x_j^i}, \quad (15)$$

where[13]

$$\frac{dx_k^i}{dp_i} = \frac{k!}{(k-d_i-1)!d_i!}p_i^{d_i}(1-p_i)^{k-d_i-1}. \quad (16)$$

From (15), we have

$$\frac{dB_i}{dp_i} < B_i\frac{1}{CW_i-\sum_{j=d_i+1}^{CW_i-1}x_j^i}\sum_{k=d_i+1}^{CW_i-1}\frac{dx_k^i}{dp_i}. \quad (17)$$

From (16) and (2), we have $dx_k^i/dp_i = k(x_k^i - x_{k-1}^i)/p_i$. Thus, (17) yields

$$\frac{dB_i}{dp_i} < \frac{B_i}{p_i}\frac{CW_i x_{CW_i-1}^i - \sum_{k=d_i+1}^{CW_i-1}x_k^i}{CW_i-\sum_{k=d_i+1}^{CW_i-1}x_k^i} \le \frac{B_i}{p_i}x_{CW_i-1}^i. \quad (18)$$

Note that

$$\begin{aligned}
&\frac{x_{CW_i-1}^i}{p_i}\\
&= \sum_{j=d_i+1}^{CW_i-1}\binom{CW_i-1}{j}p_i^{j-1}(1-p_i)^{CW_i-1-j}\\
&= \sum_{j=d_i+1}^{CW_i-1}\frac{CW_i-j}{j(1-p_i)}\binom{CW_i-1}{j-1}p_i^{j-1}(1-p_i)^{CW_i-1-(j-1)}\\
&\le \frac{CW_i-1}{2(1-p_i)}\sum_{j=d_i+1}^{CW_i-1}\binom{CW_i-1}{j-1}p_i^{j-1}(1-p_i)^{CW_i-1-(j-1)}\\
&\le \frac{CW_i-1}{2(1-p_i)} \le \frac{B_i}{1-p_i}.
\end{aligned}$$

Thus, combining the above two equations we have $dB_i/dp_i < B_i^2/(1-p_i)$. Then, $dB_i/dp_i < B_i/p_i$ follows from (18), since $x_{CW_i-1}^i \le 1$, which completes the proof. ■

Lemma 3: Let us consider the expression of τ_i as a function of p_e resulting from combining (4) with (1). According to this expression, τ_i is an increasing function of p_e.

Proof: Since $\tau_i = 1/(B_i+1)$, we need to show that $dB_i/dp_e < 0$. Note that

$$\frac{dB_i}{dp_e} = \frac{dB_i}{dp_i}\frac{dp_i}{dp_e}. \quad (19)$$

From $p_i = 1 - p_e/(1-\tau_i) = 1 - p_e(B_i+1)/B_i$, we have

$$\frac{dp_i}{dp_e} = -\frac{B_i+1}{B_i} + \frac{p_e}{B_i^2}\frac{dB_i}{dp_e}. \quad (20)$$

Combining (19) and (20) yields

$$\frac{dB_i}{dp_e} = -\frac{dB_i}{dp_i}\frac{B_i+1}{B_i}\frac{1}{1-\frac{p_e}{B_i^2}\frac{dB_i}{dp_i}}. \quad (21)$$

Let us distinguish two cases to prove this lemma, one for $p_i = 1$ and the other for $0 \le p_i < 1$. First, for $p_i = 1$, we have $p_e = 0$ from (1). Thus, (21) is smaller than 0.

[13]To compute dx_k^i/dp_i, we observe that x_k^i is the complementary cumulative function of a binomial distribution.

We now look at the case $0 \le p_i < 1$. From Lemma 2, we have $dB_i/dp_i > 0$ therefore, $dB_i/dp_e < 0$ as long as

$$\frac{dB_i}{dp_i} < \frac{B_i^2}{p_e} = \frac{B_i(B_i+1)}{1-p_i}. \quad (22)$$

According to Corollary 2, $dB_i/dp_i < B_i^2/(1-p_i)$, which is a sufficient condition for (22). This terminates the proof. ■

The following lemmas relate to the stationary regime of (7). Let $\Phi(p_e) = \prod_{k=0}^{m-1}(1-\tau_k(p_e))^{\hat{n}_k(p_e)}$. The following lemmas examine the function $\Phi(p_e)$, where each $\hat{n}_k(p_e)$ is a function of $\beta_i(p_e)$, $p_i(p_e)$, $\tau_i(p_e)$, $0 \le i \le m-1$, as given by (EQ).

Lemma 4: Let $\Phi(p_e) = \prod_{k=0}^{m-1}(1-\tau_k(p_e))^{\hat{n}_k(p_e)}$. Then, if (COND) is satisfied, $\partial\Phi/\partial\beta_j > 0$, for any $0 \le j < m-1$.

Proof: The reader is referred to [1] for the proof of this lemma. Note that, while [1] requires $CW_{i+1} \ge 2CW_i - d_i - 1$, here we only require that (COND) is satisfied, which allows for a wider range of configurations. In spite of this difference, the proof of both lemmas is identical. ■

Lemma 5: Let $\Phi(p_e) = \prod_{k=0}^{m-1}(1-\tau_k(p_e))^{\hat{n}_k(p_e)}$. Then, if (COND) is satisfied, $\partial\Phi/\partial p_j > 0$, for any $0 \le j \le m-1$.

Proof: The reader is referred to [1] for the proof of this lemma. The comment of Lemma 4 also applies to this one. ■

Lemma 6: Let $\Phi(p_e) = \prod_{k=0}^{m-1}(1-\tau_k(p_e))^{\hat{n}_k(p_e)}$. Then, if (COND) is satisfied, $\partial\Phi/\partial\tau_j < 0$, for any $0 \le j \le m-1$.

Proof: The reader is referred to [1] for the proof of this lemma. The comment of Lemma 4 also applies to this one. ■

Lemma 7: Let $j_i(p_i) \doteq \tau_i(p_i)p_i + \beta(p_i)$. Then $dj_i/dp_i \le 1$.

Proof: Let us define $J_i \doteq 1/j_i$. Then, from (4) and (5), it can be seen that

$$J_i = \frac{\sum_{k=d_i+1}^{CW_i-1}\Big((k+1)(1-x_k^i)+\sum_{j=d_i+1}^{k}j(x_j^i-x_{j-1}^i)\Big)}{CW_i-\sum_{k=d_i+1}^{CW_i-1}(1-x_k^i)(1-p_i)}. \quad (23)$$

An equivalent expression for J_i is as follows

$$\begin{aligned}
J_i = &\frac{1}{CW_i}\sum_{k=d_i+1}^{CW_i-1}(1-x_k^i)(1-p_i)J_i + \frac{CW_i-1}{2}\\
&-\frac{1}{CW_i}\sum_{k=d_i+1}^{CW_i-1}\sum_{j=d_i+1}^{k}x_j^i. \quad (24)
\end{aligned}$$

By derivation of the above expression, we obtain

$$\begin{aligned}
\frac{dJ_i}{dp_i} = &\frac{1}{CW_i}\sum_{k=d_i+1}^{CW_i-1}(1-x_k^i)(1-p_i)\frac{dJ_i}{dp_i}\\
&-\frac{1}{CW_i}J_i\sum_{k=d_i+1}^{CW_i-1}\frac{dx_k^i}{dp_i}(1-p_i)+(1-x_k^i)\\
&-\frac{1}{CW_i}\sum_{k=d_i+1}^{CW_i-1}\sum_{j=d_i+1}^{k}\frac{dx_j^i}{dp_i}.
\end{aligned}$$

From the above

$$-\frac{dJ_i}{dp_i} = \frac{\sum_{k=d_i+1}^{CW_i-1}\Big(J_i\big(\frac{dx_k^i}{dp_i}(1-p_i)+(1-x_k^i)\big)+\sum_{j=d_i+1}^{k-1}\frac{dx_j^i}{dp_i}\Big)}{CW_i-\sum_{k=d_i+1}^{CW_i-1}(1-p_i)(1-x_k^i)}.$$

Note that $dx_j^i/dp_i = j(x_j^i - x_{j-1}^i)/p_i$. Furthermore, it holds $J_i \geq 1/p_i$. This can be seen as follows. For $d_i = 0$ it can be seen from (24) that J_i is equal to the average of a geometric random variable of probability p_i. By rewriting (23) as follows, it can also be seen that J_i becomes larger as d_i increases (indeed, when d_i increases, the terms x_j^i decrease for all j, and hence the numerator increases and the denominator decreases):

$$J_i = \frac{\sum_{k=d_i+1}^{CW_i-1}\left((k+1) - \sum_{j=d_i+1}^{k} x_j^i\right)}{CW_i - \sum_{k=d_i+1}^{CW_i-1}(1-x_k^i)(1-p_i)}. \tag{25}$$

Therefore, $J_i = 1/p_i$ for $d_i = 0$ and $J_i > 1/p_i$ for any other d_i. From this,

$$-\frac{dJ_i}{dp_i} \leq \frac{J_i \sum_{k=d_i+1}^{CW_i-1}\left(\frac{dx_k^i}{dp_i}(1-p_i) + (1-x_k^i) + \sum_{j=d_i+1}^{k-1} j(x_j^i - x_{j-1}^i)\right)}{CW_i - \sum_{k=d_i+1}^{CW_i-1}(1-p_i)(1-x_k^i)}. \tag{26}$$

Recall that $1 - x_k^i$ is the probability of the event that there have been d_i or fewer transmissions in k time slots, from which

$$1 - x_k^i \geq \frac{k!}{(k-d_i)!d_i!} p_i^{d_i}(1-p_i)^{k-d_i}.$$

From the above and (16), we have

$$1 - x_k^i \geq \left(\frac{1-p_i}{k-d_i}\right)\frac{dx_k^i}{dp_i} \geq \frac{1-p_i}{k}\frac{dx_k^i}{dp_i}$$

hence, $(1-p_i)dx_k^i/dp_i \leq k(1-x_k^i)$.

Combining the above with (26) yields

$$-\frac{dJ_i}{dp_i} \leq \frac{J_i \sum_{k=d_i+1}^{CW_i-1}\left((k+1)(1-x_k^i) + \sum_{j=d_i+1}^{k-1} j(x_j^i - x_{j-1}^i)\right)}{CW_i - \sum_{k=d_i+1}^{CW_i-1}(1-p_i)(1-x_k^i)},$$

and combining the above with (23) we obtain $-dJ_i/dp_i \leq J_i^2$, which proves the lemma due to $j_i = 1/J_i$. ∎

Lemma 8: Let $\gamma = \tau_0 y_0 + \tau_1 y_1 + \tau_2(1-y_0-y_1)$. If (COND) is satisfied, it holds that $0 < \partial\gamma/\partial y_i \leq \tau_i$.

Proof: The partial derivative can be expressed as

$$\begin{aligned}\frac{\partial\gamma}{\partial y_i} &= \frac{\partial}{\partial y_i}\left(\tau_0 y_0 + \tau_1 y_1 + \tau_2(1-y_0-y_1)\right)\\ &= \tau_i - \tau_2 + y_0\frac{\partial\tau_0}{\partial\gamma}\frac{\partial\gamma}{\partial y_i} + y_1\frac{\partial\tau_1}{\partial\gamma}\frac{\partial\gamma}{\partial y_i}\\ &\quad + (1-y_0-y_1)\frac{\partial\tau_2}{\partial\gamma}\frac{\partial\gamma}{\partial y_i},\end{aligned} \tag{27}$$

from which

$$\frac{\partial\gamma}{\partial y_i} = \frac{\tau_i - \tau_2}{1 - y_0\frac{\partial\tau_0}{\partial\gamma} - y_1\frac{\partial\tau_1}{\partial\gamma} - (1-y_0-y_1)\frac{\partial\tau_2}{\partial\gamma}}. \tag{28}$$

From Lemma 2, we have that τ_i is a decreasing function of $\rho = 1 - e^{-\gamma}$, and hence $\partial\tau_i/\partial\gamma \leq 0$. Furthermore, due to (COND), we have $\tau_i - \tau_2 > 0$ for $i = 0, 1$. Combining this with (28) yields $\partial\gamma/\partial y_i > 0$. Now, combining (27) with $\partial\tau_i/\partial\gamma \leq 0$ and $\partial\gamma/\partial y_i \geq 0$ yields $\partial\gamma/\partial y_i \leq \tau_i$. ∎

Proof of Theorem 5: For $m = 3$, the system (ODE) can be expressed with the following two equations as a function of y_0 and y_1 (where $y_2 = 1 - y_0 - y_1$):

$$\begin{aligned}\frac{dy_0}{dt} &= \gamma e^{-\gamma} - y_0(\tau_0 + \beta_0) = f_0(y_0, y_1)\\ \frac{dy_1}{dt} &= y_0(\tau_0(1-e^{-\gamma}) + \beta_0) - y_1(\tau_1 + \beta_1) = f_1(y_0, y_1).\end{aligned}$$

where $\gamma = \tau_0 y_0 + \tau_1 y_1 + \tau_2(1-y_0-y_1)$ (to simplify notation, we have omitted the dependency of τ_i and β_i on γ in the above equations).

According to the Markus-Yamabe theorem,[14] the above system is globally asymptotically stable if the real part of the eigenvalues of the following Jacobian matrix are negative for all points (y_0, y_1):

$$\begin{pmatrix}\frac{\partial f_0}{\partial y_0} & \frac{\partial f_0}{\partial y_1}\\ \frac{\partial f_1}{\partial y_0} & \frac{\partial f_1}{\partial y_1}\end{pmatrix}.$$

The characteristic polynomial of the matrix is given by

$$\lambda^2 - (c_{00} + c_{11})\lambda + c_{00}c_{11} - c_{01}c_{10},$$

where $c_{ij} = \partial f_i/\partial y_j$.

According to the Routh-Hurwitz stability criterion, as long as the following two inequalities are satisfied, the real part of the eigenvalues of the above characteristic polynomial are guaranteed to be negative:

$$-(c_{00} + c_{11}) > 0, \tag{29}$$

$$c_{00}c_{11} - c_{01}c_{10} > 0. \tag{30}$$

Sufficient conditions for (29) are (i) $c_{00} < 0$ and (ii) $c_{11} < 0$, and sufficient conditions for (30) are: (iii) $-c_{00} > c_{10}$, (iv) $-c_{11} > c_{01}$ and (v) c_{10} and c_{01} are never negative simultaneously. In the following, we show that each of these five conditions is satisfied.

Condition (i): $c_{00} < 0$.

$$\begin{aligned}c_{00} = \frac{\partial f_0}{dy_0} &= (1-\gamma)e^{-\gamma}\frac{\partial\gamma}{\partial y_0} - (\tau_0 + \beta_0)\\ &\quad - y_0\frac{\partial(\tau_0+\beta_0)}{\partial(1-e^{-\gamma})}\frac{\partial(1-e^{-\gamma})}{\partial\gamma}\frac{\partial\gamma}{\partial y_0}.\end{aligned} \tag{31}$$

Removing some negative terms from the above equation and considering that $\partial(\tau_0+\beta_0)/\partial(1-e^{-\gamma}) > 0$, $\partial\gamma/\partial y_0 > 0$ (see Lemma 8) and $(1-\gamma)e^{-\gamma} < 1$, we obtain the following upper bound on c_{00}:

$$c_{00} < \frac{\partial\gamma}{\partial y_0} - \tau_0.$$

From Lemma 8, the left-hand side of the above is smaller than or equal to 0.

Condition (ii): $c_{11} < 0$.

$$\begin{aligned}c_{11} &= y_0\frac{\partial(\tau_0(1-e^{-\gamma})+\beta_0)}{\partial(1-e^{-\gamma})}\frac{\partial(1-e^{-\gamma})}{\partial\gamma}\frac{\partial\gamma}{\partial y_1}\\ &\quad - (\tau_1+\beta_1) - y_1\frac{\partial(\tau_1+\beta_1)}{\partial(1-e^{-\gamma})}\frac{\partial(1-e^{-\gamma})}{\partial\gamma}\frac{\partial\gamma}{\partial y_1}\\ &\leq y_0\frac{\partial(\tau_0(1-e^{-\gamma})+\beta_0)}{\partial(1-e^{-\gamma})}\frac{\partial(1-e^{-\gamma})}{\partial\gamma}\frac{\partial\gamma}{\partial y_1} - \tau_1.\end{aligned}$$

[14]This theorem was initially stated as a conjecture for any n, and was later proved to be true for $n = 2$ (which is the case here) and false for $n > 2$ [20].

From Lemmas 7 and 8, and $e^{-\gamma} < 1$, we obtain the following upper bound

$$c_{11} < y_0\tau_1 - \tau_1 \leq 0.$$

Condition (iii): $-c_{00} > c_{10}$.

We have

$$\begin{aligned} c_{10} = \tau_0 + \beta_0 + y_0 \frac{\partial(\tau_0+\beta_0)}{\partial(1-e^{-\gamma})}\frac{\partial(1-e^{-\gamma})}{\partial\gamma}\frac{\partial\gamma}{\partial y_0} - e^{-\gamma}\tau_0 \\ - y_0 \frac{\partial(e^{-\gamma}\tau_0)}{\partial(1-e^{-\gamma})}\frac{\partial(1-e^{-\gamma})}{\partial\gamma}\frac{\partial\gamma}{\partial y_0} \\ - y_1 \frac{\partial(\tau_1+\beta_1)}{\partial(1-e^{-\gamma})}\frac{\partial(1-e^{-\gamma})}{\partial\gamma}\frac{\partial\gamma}{\partial y_0}. \end{aligned}$$

Comparing the above equation with (31), it can be seen that it holds $-c_{00} > c_{10}$ as long as

$$\begin{aligned} -(1-\gamma)e^{-\gamma}\frac{\partial\gamma}{\partial y_0} \\ > -e^{-\gamma}\tau_0 - y_0 \frac{\partial(e^{-\gamma}\tau_0)}{\partial(1-e^{-\gamma})}\frac{\partial(1-e^{-\gamma})}{\partial\gamma}\frac{\partial\gamma}{\partial y_0} \\ - y_1 \frac{\partial(\tau_1+\beta_1)}{\partial(1-e^{-\gamma})}\frac{\partial(1-e^{-\gamma})}{\partial\gamma}\frac{\partial\gamma}{\partial y_0}. \end{aligned}$$

Removing some terms and rearranging others, we obtain the following sufficient condition for the above

$$e^{-\gamma}\left(\tau_0 - \frac{\partial\gamma}{\partial y_0}\right) > -\gamma e^{-\gamma}\frac{\partial\gamma}{\partial y_0} - y_0\frac{\partial(e^{-\gamma}\tau_0)}{\partial\gamma}\frac{\partial\gamma}{\partial y_0}.$$

Following a similar reasoning to Lemma 8, it can be seen that $\partial\gamma/\partial y_0 < \tau_0 + y_0\partial\tau_0/\partial y_0$, from which we obtain the following sufficient condition

$$-e^{-\gamma}y_0\frac{\partial\tau_0}{\partial y_0} > -\gamma e^{-\gamma}\frac{\partial\gamma}{\partial y_0} - y_0\frac{\partial(e^{-\gamma}\tau_0)}{\partial\gamma}\frac{\partial\gamma}{\partial y_0}.$$

Taking into account that $\frac{\partial\tau_0}{\partial y_0} = \frac{\partial\tau_0}{\partial\gamma}\frac{\partial\gamma}{\partial y_0}$, this is equivalent to

$$-e^{-\gamma}y_0\frac{\partial\tau_0}{\partial\gamma} > -\gamma e^{-\gamma} - y_0\frac{\partial(e^{-\gamma}\tau_0)}{\partial\gamma}.$$

Operating on the above we obtain

$$-e^{-\gamma}y_0\frac{\partial\tau_0}{\partial\gamma} > -\gamma e^{-\gamma} - y_0e^{-\gamma}\frac{\partial\tau_0}{\partial\gamma} + y_0e^{-\gamma}\tau_0.$$

The above is equivalent to

$$0 > -e^{-\gamma}(\gamma - y_0\tau_0),$$

which is true given that $\gamma > y_0\tau_0$ for $y_0 < 1$ (for the case $y_0 = 1$ it can be seen that this condition also holds).

Condition (iv): $-c_{11} > c_{01}$.

A sufficient condition for this case is given by

$$\begin{aligned} y_0\frac{\partial(e^{-\gamma}\tau_0)}{\partial\gamma}\frac{\partial\gamma}{\partial y_1} + (\tau_1+\beta_1) + y_1\frac{\partial(\tau_1+\beta_1)}{\partial\gamma}\frac{\partial\gamma}{\partial y_1} \\ > (1-\gamma)e^{-\gamma}\frac{\partial\gamma}{\partial y_1}. \end{aligned} \tag{32}$$

The left-hand side of (32) is lower bounded by

$$\tau_1 - y_0e^{-\gamma}\tau_0\frac{\partial\gamma}{\partial y_1} + y_0e^{-\gamma}\frac{\partial\tau_0}{\partial\gamma}\frac{\partial\gamma}{\partial y_1}.$$

Given $\frac{\partial\tau_0}{\partial\gamma}\frac{\partial\gamma}{\partial y_1} = \frac{\partial\tau_0}{\partial y_1}$ and $\frac{\partial\gamma}{\partial y_1} < \tau_1$, the above is lower bounded by

$$\begin{aligned} \tau_1 - y_0e^{-\gamma}\tau_0\tau_1 + y_0e^{-\gamma}\frac{\partial\tau_0}{\partial y_1} \\ = \tau_1e^{-\gamma}(1-y_0\tau_0) + \tau_1(1-e^{-\gamma}) + \frac{\partial\tau_0}{\partial y_1}y_0e^{-\gamma}. \end{aligned}$$

From $1 - e^{-x} > xe^{-x}$, the above is lower bounded by

$$\tau_1e^{-\gamma}(1-y_0\tau_0) + \tau_1\gamma e^{-\gamma} + \frac{\partial\tau_0}{\partial y_1}y_0e^{-\gamma}. \tag{33}$$

It can be seen that $0 > \partial\tau_0/\partial\gamma > -1$. From the proof of Corollary 2, $\frac{\partial B_0}{\partial(1-e^{-\gamma})} \leq \frac{B_0^2}{e^{-\gamma}}$, where $B_0 = \frac{1}{\tau_0} - 1$. Thus,

$$\frac{\partial\tau_0}{\partial\gamma} = -\frac{1}{(B_0+1)^2}\frac{\partial B_0}{\partial(1-e^{-\gamma})}\frac{\partial(1-e^{-\gamma})}{\partial\gamma} > -1. \tag{34}$$

Combining this with Lemma 8 yields $|\partial\tau_0/\partial y_1| < \tau_1$, from which $\tau_1\gamma e^{-\gamma} > -\gamma e^{-\gamma}y_0\frac{\partial\tau_0}{\partial y_1}$. Combining this with (33) yields the following lower bound for the LHS of (32)

$$\tau_1e^{-\gamma}(1-y_0\tau_0) + \frac{\partial\tau_0}{\partial y_1}y_0e^{-\gamma}(1-\gamma). \tag{35}$$

From $\partial\gamma/\partial y_1 < \tau_1 + y_0\partial\tau_0/\partial y_1$, the right-hand side of (32) is upper bounded by

$$(1-\gamma)e^{-\gamma}\tau_1 + (1-\gamma)e^{-\gamma}y_0\frac{\partial\tau_0}{\partial y_1}. \tag{36}$$

Comparing (35) with (36), it can be seen that that in (35) the positive term is larger and the negative terms are equal, which implies that (32) is satisfied.

Condition (v): either $c_{10} \geq 0$ *or* $c_{01} \geq 0$.

To show that c_{10} and c_{01} are never negative simultaneously, we prove that when $y_0 < 1-\gamma$ it holds $c_{01} \geq 0$, and otherwise $c_{10} \geq 0$. Let us start with c_{01},

$$\begin{aligned} c_{01} &= (1-\gamma)e^{-\gamma}\frac{\partial\gamma}{\partial y_1} - y_0\frac{\partial(\tau_0+\beta_0)}{\partial(1-e^{-\gamma})}\frac{\partial(1-e^{-\gamma})}{\partial\gamma}\frac{\partial\gamma}{\partial y_1} \\ &= (1-\gamma)e^{-\gamma}\frac{\partial\gamma}{\partial y_1} - y_0\frac{\partial(\tau_0(1-e^{-\gamma})+\beta_0)}{\partial(1-e^{-\gamma})}e^{-\gamma}\frac{\partial\gamma}{\partial y_1} \\ &\quad - y_0\frac{\partial(\tau_0e^{-\gamma})}{\partial(1-e^{-\gamma})}e^{-\gamma}\frac{\partial\gamma}{\partial y_1}. \end{aligned}$$

Given that τ_0 is a decreasing function of $1-e^{-\gamma}$ (Lemma 2), the last term of the above expression is positive, hence

$$c_{01} \geq (1-\gamma)e^{-\gamma}\frac{\partial\gamma}{\partial y_1} - y_0\frac{\partial(\tau_0(1-e^{-\gamma})+\beta_0)}{\partial(1-e^{-\gamma})}e^{-\gamma}\frac{\partial\gamma}{\partial y_1}.$$

By combining the above with Lemma 7, we obtain

$$c_{01} \geq \left((1-\gamma)e^{-\gamma} - y_0e^{-\gamma}\right)\frac{\partial\gamma}{\partial y_1},$$

which is larger than or equal to 0 as long as $y_0 < 1-\gamma$.

We now look at c_{10} when $y_0 > 1-\gamma$,

$$\begin{aligned} &c_{10} \\ &= \tau_0(1-e^{-\gamma}) + \beta_0 + y_0\frac{\partial(\tau_0(1-e^{-\gamma})+\beta_0)}{\partial(1-e^{-\gamma})} \\ &\quad \cdot\frac{\partial(1-e^{-\gamma})}{\partial\gamma}\frac{\partial\gamma}{\partial y_0} - y_1\frac{\partial(\tau_1+\beta_1)}{\partial(1-e^{-\gamma})}\frac{\partial(1-e^{-\gamma})}{\partial\gamma}\frac{\partial\gamma}{\partial y_0} \\ &= \tau_0(1-e^{-\gamma}) + \beta_0 + y_0\frac{\partial(\tau_0(1-e^{-\gamma})+\beta_0)}{\partial(1-e^{-\gamma})}\frac{\partial(1-e^{-\gamma})}{\partial\gamma} \end{aligned}$$

$$\cdot \frac{\partial \gamma}{\partial y_0} - y_1 \frac{\partial(\tau_1(1-e^{-\gamma})+\beta_1)}{\partial(1-e^{-\gamma})} \frac{\partial(1-e^{-\gamma})}{\partial \gamma} \frac{\partial \gamma}{\partial y_0}$$
$$- y_1 \frac{\partial \tau_1 e^{-\gamma}}{\partial(1-e^{-\gamma})} \frac{\partial(1-e^{-\gamma})}{\partial \gamma} \frac{\partial \gamma}{\partial y_0} \geq \tau_0(1-e^{-\gamma})$$
$$- y_1 \frac{\partial(\tau_1(1-e^{-\gamma})+\beta_1)}{\partial(1-e^{-\gamma})} \frac{\partial(1-e^{-\gamma})}{\partial \gamma} \frac{\partial \gamma}{\partial y_0}.$$

From Lemma 7 we obtain the following inequality

$$c_{10} \geq \tau_0(1-e^{-\gamma}) - y_1 e^{-\gamma} \tau_0.$$

Given $y_0 > 1-\gamma$, we have $y_1 \leq 1-y_0 < \gamma$. Substituting this into the above equation yields

$$c_{10} \geq \tau_0(1-e^{-\gamma}) - \tau_0 \gamma e^{-\gamma},$$

which is larger than 0 given that $1-e^{-x} > xe^{-x}$. ■

ACKNOWLEDGEMENTS

The authors thank the editor and reviewers for their valuable feedback, which has been very helpful in improving the paper.

REFERENCES

[1] C. Vlachou, A. Banchs, J. Herzen, and P. Thiran, "On the MAC for power-line communications: Modeling assumptions and performance tradeoffs," in *Proc. IEEE 22nd ICNP*, Raleigh, NC, USA, Oct. 2014, pp. 456–467.

[2] *HomePlug Alliance*, accessed on Jun. 12, 2016. [Online]. Available: www.homeplug.org

[3] *nVoy Hybrid Networking*, accessed on Jun. 12, 2016. [Online]. Available: http://www.nvoy.org/

[4] *IEEE Standard for Broadband Over Power Line Networks: Medium Access Control and Physical Layer Specifications*, IEEE Standard 1901, 2010.

[5] G. Bianchi, "Performance analysis of the IEEE 802.11 distributed coordination function," *IEEE J. Sel. Areas Commun.*, vol. 18, no. 3, pp. 535–547, Mar. 2000.

[6] M. Y. Chung, M.-H. Jung, T.-J. Lee, and Y. Lee, "Performance analysis of HomePlug 1.0 MAC with CSMA/CA," *IEEE J. Sel. Areas Commun.*, vol. 24, no. 7, pp. 1411–1420, Jul. 2006.

[7] C. Vlachou, A. Banchs, J. Herzen, and P. Thiran, "Performance analysis of MAC for power-line communications," in *Proc. ACM SIGMETRICS*, Austin, TX, USA, Jun. 2014, pp. 585–586.

[8] C. Cano and D. Malone, "On efficiency and validity of previous HomePlug MAC performance analysis," *Comput. Netw.*, vol. 83, pp. 118–135, Jun. 2015.

[9] A. Kumar, E. Altman, D. Miorandi, and M. Goyal, "New insights from a fixed-point analysis of single cell IEEE 802.11 WLANs," *IEEE/ACM Trans. Netw.*, vol. 15, no. 3, pp. 588–601, Jun. 2007.

[10] J.-W. Cho, J.-Y. Le Boudec, and Y. Jiang, "On the asymptotic validity of the decoupling assumption for analyzing 802.11 MAC protocol," *IEEE Trans. Inf. Theory*, vol. 58, no. 11, pp. 6879–6893, Nov. 2012.

[11] K. Huang, K. R. Duffy, and D. Malone, "On the validity of IEEE 802.11 MAC modeling hypotheses," *IEEE/ACM Trans. Netw.*, vol. 18, no. 6, pp. 1935–1948, Dec. 2010.

[12] G. Sharma, A. Ganesh, and P. Key, "Performance analysis of contention based medium access control protocols," *IEEE Trans. Inf. Theory*, vol. 55, no. 4, pp. 1665–1682, Apr. 2009.

[13] C. Vlachou, A. Banchs, J. Herzen, and P. Thiran, "Analyzing and boosting the performance of power-line communication networks," in *Proc. ACM CoNEXT*, Sydney, NSW, Australia, Dec. 2014, pp. 1–12.

[14] C. Bordenave, D. McDonald, and A. Proutiere, "A particle system in interaction with a rapidly varying environment: Mean field limits and applications," *Netw. Heterogeneous Media*, vol. 5, no. 1, pp. 535–547, 2010.

[15] M. Benaïm and J.-Y. Le Boudec, "A class of mean field interaction models for computer and communication systems," *Perform. Eval.*, vol. 65, nos. 11–12, pp. 823–838, 2008.

[16] C. Vlachou, J. Herzen, and P. Thiran, "Simulator and experimental framework for the MAC of power-line communications," EPFL, Lausanne, Switzerland, EPFL Tech. Rep. 205770, 2014. [Online]. Available: https://infoscience.epfl.ch/

[17] *OpenWrt*, accessed on Jun. 12, 2016. [Online]. Available: https://openwrt.org/

[18] *Qualcomm Atheros Open Powerline Toolkit*, accessed on Jun. 12, 2016. [Online]. Available: https://github.com/qca/open-plc-utils

[19] V. Ramaiyan, A. Kumar, and E. Altman, "Fixed point analysis of single cell IEEE 802.11e WLANs: Uniqueness and multistability," *IEEE/ACM Trans. Netw.*, vol. 16, no. 5, pp. 1080–1093, Oct. 2008.

[20] R. Feßler, "A proof of the two-dimensional Markus–Yamabe stability conjecture and a generalization," *Ann. Pol. Math.*, vol. 62, no. 1, pp. 45–75, 1995.

Christina Vlachou received the Diploma degree in electrical and computer engineering from the National Technical University of Athens in 2011, and the Ph.D. degree from EPFL in 2016. Her dissertation focuses on measuring, modeling, and enhancing power-line communications (PLC) performance. Her Ph.D. thesis has been nominated for the EPFL Doctorate Award and her work on PLC has received the Best Paper Runner-Up Award at the IEEE ICNP 2014 Conference. During her Ph.D. studies, she interned with Marvell and Qualcomm. She received the Papakyriakopoulos Award for excellence in Mathematics, in 2007, from the National Technical University of Athens. Her interests include wireless and mobile communications, multiuser performance, and design of heterogeneous networks.

Albert Banchs (M'04–SM'12) received the M.Sc. and Ph.D. degrees from the Polytechnic University of Catalonia in 1997 and 2002, respectively. He was with ICSI Berkeley in 1997, Telefonica I+D in 1998, and NEC Europe Ltd. from 1998 to 2003. He is currently a Professor with the University Carlos III of Madrid and has a double affiliation as a Deputy Director of the IMDEA Networks Institute. His research interests include the performance evaluation and algorithm design in wireless and wired networks. He is an Editor of the IEEE TRANSACTIONS ON WIRELESS COMMUNICATIONS, and the Green Communications and Networking Series of the IEEE JOURNAL OF SELECTED AREAS IN COMMUNICATIONS. He serves as the Co-Chair of the third International Workshop on 5G Architecture (2016).

Julien Herzen received the M.Sc. degree in communication systems and the Ph.D. degree from EPFL in 2009 and 2015, respectively. From 2009 to 2012, he interned with Docomo Innovations, Deutsche Telekom, and Technicolor. He is currently a Data Scientist with the Big Data and Network Intelligence Group, Swisscom. His research interests are in data analytics and in the design and analysis of network and graph algorithms. He received the best paper award at ACM COSN 2014 and was a co-recipient of the Runner-Up Best Paper Award at the IEEE ICNP 2014. His Ph.D. thesis has been nominated for the Patrick Denantes Memorial Award.

Patrick Thiran (S'89–M'96–SM'12–F'14) received the Electrical Engineering degree from the Université Catholique de Louvain, Louvain-la-Neuve, Belgium, in 1989, the M.S. degree in electrical engineering from the University of California at Berkeley, USA, in 1990, and the Ph.D. degree from EPFL in 1996. He became an Adjunct Professor in 1998, an Assistant Professor in 2002, an Associate Professor in 2006, and a Full Professor in 2011. From 2000 to 2001, he was with Sprint Advanced Technology Labs, Burlingame, CA. He is currently a Full Professor with EPFL. He is active in the analysis and design of wireless and PLC networks, in network measurements, and in data-driven network science. His research interests include networks, performance analysis, and stochastic models. He served as an Associate Editor of the IEEE TRANSACTIONS ON CIRCUITS AND SYSTEMS from 1997 to 1999, and the IEEE/ACM TRANSACTIONS ON NETWORKING from 2006 to 2010. He is currently serving on the Editorial Board of the IEEE JOURNAL ON SELECTED AREAS IN COMMUNICATION. He was a recipient of the 1996 EPFL Ph.D. Award and the 2008 Crédit Suisse Teaching Award.